JOURNAL OF MATERIALS SCIENCE **38** (2003) 2883–2891

Selective case hardening of plain steel by carbon alloying with a plasma transferred arc (PTA) technique

J. NIKOLAOU, L. BOURITHIS, G.PAPADIMITRIOU
Laboratory of Physical Metallurgy, National Technical University of Athens, 9 Iroon Polytechniou Street, Zographou Campus, 15780-Athens, Greece
E-mail: geopapad@metal.ntua.gr

The present work was undertaken in order to study the possibility of case hardening of a plain steel using the Plasma Transferred Arc (PTA) alloying process. It was found that, depending on the PTA operation parameters and cooling rates, either carburizing or case hardening can be obtained. The depth of carburizing reaches a depth up to 1 mm and can be pre-selected by adjusting the PTA operation parameters. Due to the beneficial effect of carburizing with the PTA alloying technique, wear resistance of the treated surface is significantly improved.

1. Introduction

Low-carbon steels, which are readily machinable, can have their surface layers carburized and subsequently hardened. The treatment, called case hardening, gives the steel a hard and wear resistant surface or case. By virtue of the fact that the core remains comparatively soft and tough the component as a whole shows high impact strength. Owing to the development of compressive stresses in the surface layers during the case-hardening treatment the fatigue strength of the steel is also improved [1].

The most important methods of carburizing fall broadly into three categories: by pack carburizing, liquid carburizing and gas carburizing [2]. In addition, two relative new techniques have been introduced for carburizing steels, vacuum carburizing and plasma carburizing, with the advantage of achieving a higher concentration of carbon on the surface of the steel and minimizing the carburizing time which, generally speaking, is very high when using the previous techniques [2]. But all these techniques have two main disadvantages. First the workpiece is heated to high temperatures for a considerable period of time and second for selective carburizing the workpiece needs additional treatment [1].

To overcome these two disadvantages the laser beam alloying technique has been employed [3]. With this technique the surface of the steel is covered with a graphite coating, then the laser beam scans the surface and the carburizing takes place with two possible mechanisms. The first mechanism involves the melting of a surface layer of the steel and the mixing of the carbon coating with the melt producing the carburized layer [4–7]. The second mechanism involves diffusion of carbon in the solid state (no melting of the substrate takes place) activated by laser heating [8, 9]. Although the reports on laser beam carburizing are very promising, the technique has some drawbacks. Investigators who worked with laser carburizing using the melting variant reported the formation of cracks in the carburized layer due to the brittleness of the microstructure and the high cooling rates during solidification and gas porosity in the melting zone. On the other hand the solid state diffusion technique leads to very thin carburized layers. In addition laser is a rather expensive technique. It is, therefore, interesting to investigate the plasma transferred arc process, which -despite its lower energy density- has the main advantage to require rather inexpensive equipment and the possibility to work with a higher heat input. PTA technique has proved to be as efficient as laser or electron beam in surface hardening of steels and coatings [10–19] and has been successfully tested in producing composite borided layers on tool steel surfaces [20].

In this context the present work was undertaken in order to study the possibility of case hardening of a plain steel using the PTA alloying process. Experiments were performed on steel plates by rapidly heating to peak temperatures over the melting point of steel, using both single and multiple track moving plasma arc. The geometrical characteristics (form and dimensions) of the heat affected layer and the corresponding microstructures were investigated in connection with the main process variables: heat input and plasma gas flow rate as well as cooling rate. In order to assess the wear resistance, pin on disc tests have been done on PTA alloyed specimens.

2. Procedures-experimental techniques

The substrate material used was a plate of an AISI 1522H steel of composition C: 0.2 wt%, Mn: 1.2 wt%, Si: 0.2 wt%, P: 0.015 wt%, S: 0.015 wt%, Fe (bal) in recrystallized condition. Samples of size

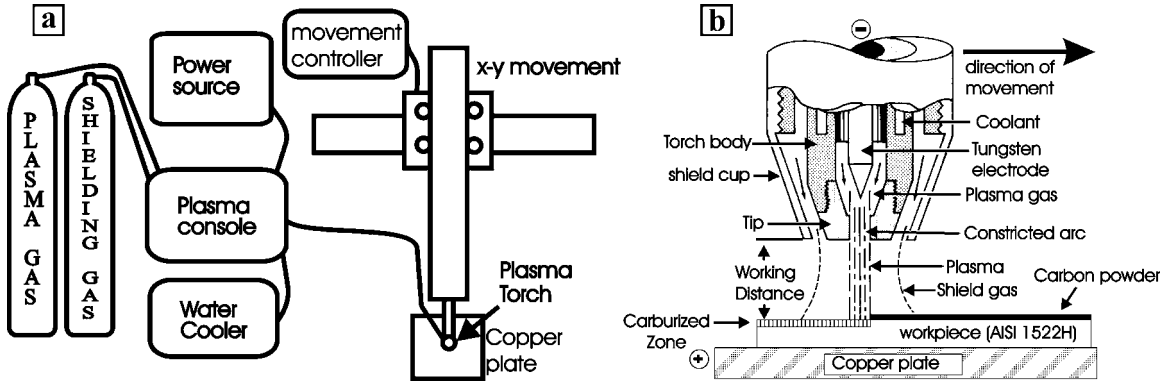

Figure 1 (a) Schematic drawing of PTA equipment used for the alloying process and (b) More detailed drawing of the PTA torch.

$50 \times 50 \times 16$ mm were cut out and polished to 120 grit emery paper. The carbon powder, having an average size of 1 μm was suspended in a solution of ethanol to produce a slurry, which was pasted directly on the specimen and then dried. The powder slurry had an average thickness of 0.03 mm and weight 0.007 gr of carbon per cm^2 of surface area.

Surface alloying was carried out by scanning the coated area with a transferred plasma arc (PTA). The main equipment employed was a PTA-2000 Sabre Arc plasma console, controlling the plasma and shielding gas flow rates, a plasma torch (PWH-3A) for low-medium current applications, a KEMPI 2000 power source and an automatic machine for control of the torch movement in the horizontal level (x-y axis). The plasma and shielding gas used was Ar with 99.99% purity and the plasma torch tip diameter was 2.01 mm. A schematic drawing of the PTA equipment used is presented in Fig. 1a and a more detailed drawing of the PTA torch in Fig. 1b.

In order to investigate the influence of the PTA working parameters on the alloying process two sets of single run experiments were performed. Different current intensities (50A–80A), plasma gas flow rate (0.2 lt/min–0.5 lt/min) and shielding gas flow rate (3.4 lt/min–7.8 lt/min), have been adopted as shown in Table I. The travelling speed of the PTA torch was kept constant at 3.0 mm/s. Microstructures and depths of alloyed layers were observed by optical and scanning electron microscopy (SEM) on polished cross-sections. Microhardness measurements of the alloyed layer were also performed using a Vickers microhardness tester with a 100 g load.

TABLE I Experimental conditions of the single run PTA passes

	Current (A)	P.G.F. (lt/min)	S.G.F. (lt/min)	Stand off distance (mm)
Series 1				
1.1	50	0.5	7.8	3.2
1.2	60	0.5	7.8	3.2
1.3	70	0.5	7.8	3.2
1.4	80	0.5	7.8	3.2
Series 2				
2.1	50	0.2	3.9	3.2
2.2	60	0.2	3.9	3.2
2.3	70	0.2	3.9	3.2
2.4	80	0.2	3.9	3.2

Based upon the preliminary results obtained with single runs, a convenient set of operation parameters was chosen for alloying the whole surface with carbon (multi-run surfaces). The amount of overlapping adopted for the PTA successive passes was 65%, in order to ensure uniform alloyed layers. Under these conditions layers with a significant thickness, free of cracks or other defects were obtained. Three cooling rates were imposed while preparing the surfaces: (i) the specimens were air-cooled (Surface A), (ii) immersed in iced water (Surface B) and (iii) in room temperature water (Surface C). The alloyed surfaces were prepared for microstructural examination using SEM and XRD and were evaluated for their wear resistance with a pin on disk apparatus.

The plasma transferred arc-alloyed surfaces (A, B and C) and an unmodified surface from the substrate material were polished up to 2000 grit emery paper and cleaned with acetone in an ultrasonic bath. The tests were conducted according to ASTM G99-95a standards under the applied load of 9.8 N and sliding velocity of 0.12 m/s. The specimens under examination were cut out from PTA carburized plates to dimensions $40 \times 40 \times 4$ mm and were placed on the rotating disk and the stationary pin was an Al_2O_3 ball with a 6 mm diameter and 1900 HV hardness. The track radius was 10 mm and the total sliding distance covered was 942 m (15000 revolutions). The pin-on-disk tracks were examined with electron microscopy in order to reveal the wear mechanisms involved.

Based on the preliminary results of the wear tests, PTA scanned surface C was chosen for more thorough wear investigation for its good wear characteristics. An additional series of pin on disk wear tests were done changing the applied load (4.9 N–19.6 N) and sliding speed (0.12 m/s–0.48 m/s). The wear tracks were also in this case examined using electron microscopy.

3. Results and discussion

3.1. Single run tests

3.1.1. Microstructure

A typical transverse section of a plasma transferred arc-treated specimen is shown in Fig. 2, which depicts the characteristic zones that form below the surface of the material after plasma treatment. When PTA irradiates a metal surface, the affected region consists of a melted

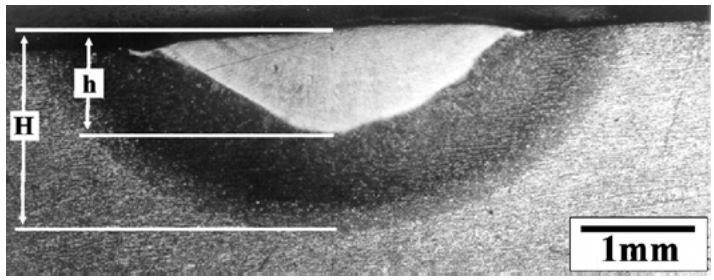

Figure 2 Optical micrograph of a cross section of a single run plasma transferred arc pass. h is the depth of the fusion zone (FZ) and H the depth of the heat affected zone (HAZ).

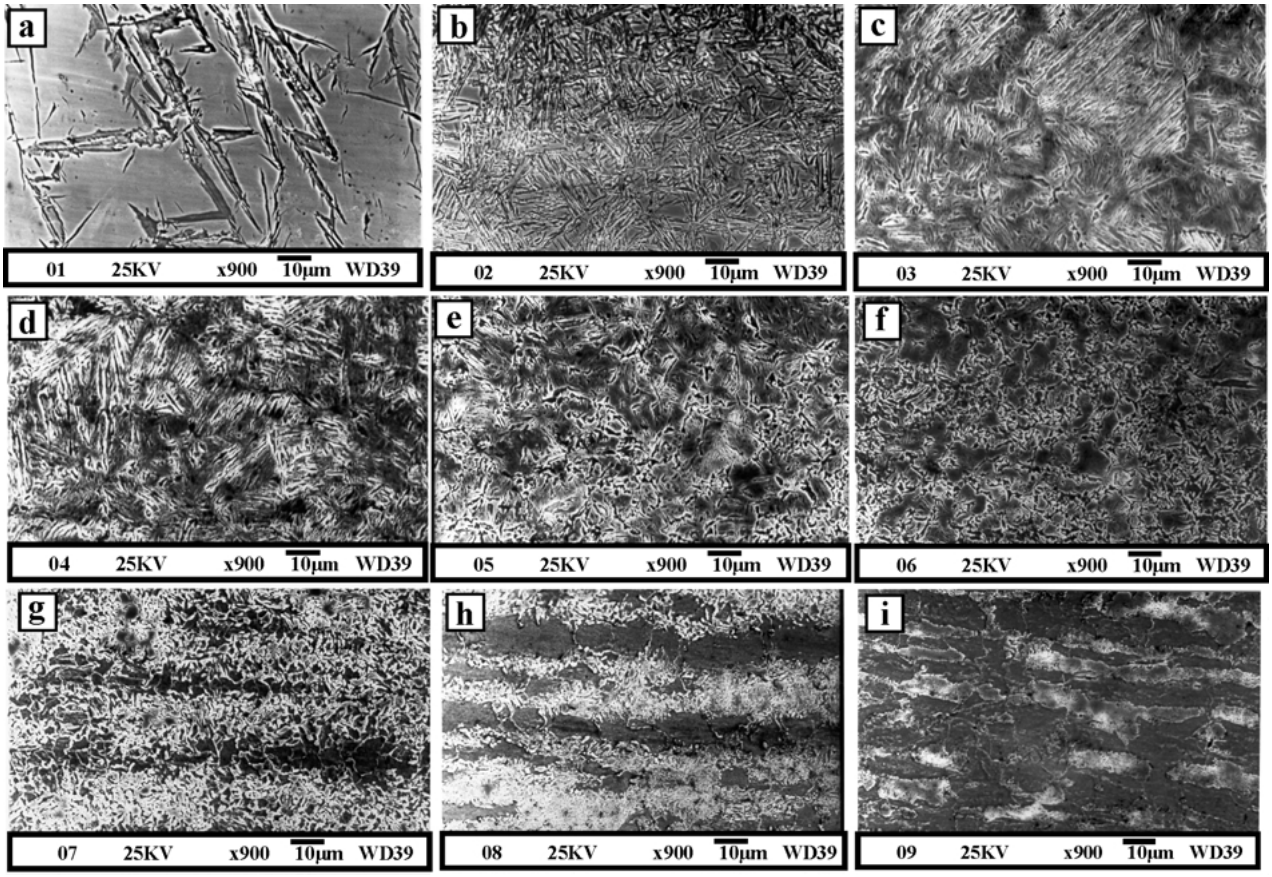

Figure 3 SEM micrographs showing the successive microstructures at increasing depth of a single run PTA pass. (a) Fusion zone, (b–h) heat affected zone, and (i) unaffected substrate steel microstructure.

fusion zone (FZ) and a heat-affected zone (HAZ). In the FZ, the metal is heated to a temperature above the melting point and alloying of the surface takes place giving a homogenized liquid phase, which is subsequently resolidified. The FZ in all single-run plasma treated surfaces consisted of plate martensite and retained austenite of volume fraction depending on the operating parameters. A typical microstructure of the FZ is shown in Fig. 3a.

In the HAZ, the metal is heated to temperatures above its transformation temperature (Ac_1). Solid-state transformations in this zone are affected by the peak temperature reached and rapid cooling rates due to self-quenching. The microstructures in HAZ is not uniform and it can be subdivided in three areas, the partial grain refining zone, the grain refining zone and the grain coarsening zone. The partial grain-refining region was subjected to peak temperatures between Ac_1 and Ac_3. The pearlite grains and a small amount of proeutectoid ferrite have been transformed into austenite which decomposes during cooling to very fine ferrite and pearlite grains. Fig. 3h and g represent the microstructure of the partial grain-refining zone for peak temperatures just above Ac_1 and just below Ac_3 respectively. In both cases a band structure is clearly observed. In the grain-refining zone the steel was subjected to peak temperatures just above Ac_3, the initially ferrite—pearlite microstructure has been transformed fully to austenite which subsequently transformed during continuous cooling into ferrite and lower bainite. This microstructure can be seen in Fig. 3e and f for different amounts of ferrite and lower bainite. Finally the peak temperatures in the grain-coarsening zone are well above Ac_3 and large austenitic grains are formed which transform during cooling into bainite and lath martensite depending on the cooling rates at this depth. Generally speaking

the higher is the peak temperature the higher is the cooling rates obtained and this explains why the microstructure changes from a mixture of lower and upper bainite to upper bainite and lath martensite as can be seen in Fig. 3d, c and b respectively. Under the HAZ the unaffected base material microstructure can be seen in Fig. 2i which consists of elongated pearlite and ferrite grains.

3.1.2. Depths of FZ and HAZ in relation to PTA parameters

The depth of the surface-alloyed layer (FZ) and the depth of HAZ depends on the PTA operating parameters as illustrated in Fig. 4. As expected higher currents lead to greater FZ and HAZ, Fig. 4a and b. The relationship between current and FZ and HAZ depths is linear within the limits examined in this work. On the other hand plasma gas flow (PGF) and shielding gas flow (SGF) rates seem to have no significant effect on the depth of the fusion zone, Fig. 4a, and have small influence on the depth of HAZ, Fig. 4b. In fact smaller PGF and SGF leads to thinner HAZ when the PTA current exceeds 60 A. This must be attributed to the fact that PGF and SGF affect the constriction of the plasma stream and thus the heat input density and hence the cooling rates achieved. The fusion zone depth (h) increases from 0.2 mm to 1.0 mm by increasing the PTA current from 50 A to 80 A.

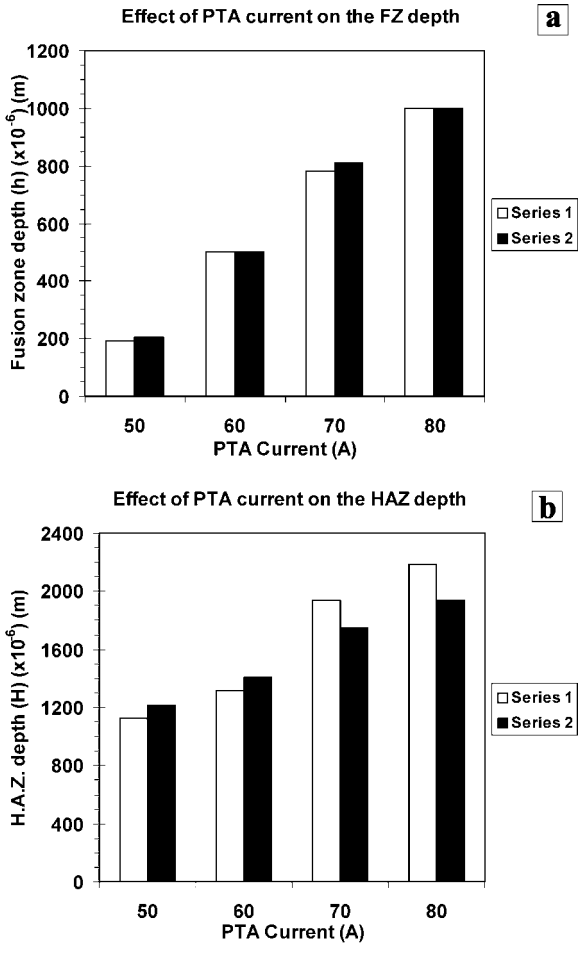

Figure 4 The effect of PTA current, plasma gas flow (PGF) and shielding gas flow (SGF) on the depth of the fusion (h) and heat affected (H) zone respectively for the operating conditions of series 1 and series 2 tests (see Table I).

3.1.3. Microhardness and PTA operating parameters

Operating plasma parameters affect both heating and cooling rates and subsequently the microstructure and hardness of the heat-treated areas. As mentioned earlier, the aim of this work was to produce hard wear resistant surfaces. Martensitic structures are required in order to achieve high hardness. The martensitic transformation primarily depends on chemical composition and cooling rate. As the substrate metal serves as a heat tank absorbing energy, the higher the specific heat input of an energy beam, the higher cooling rate is obtained.

The microhardness profiles along the depth of the alloyed layer of the series 2 of experiments (Table I) with PGF 0.2 lt/min and SGF 3.9 lt/min are illustrated in Fig. 5a. It is obvious that higher PTA current leads to higher hardness of the fusion zone. Since the mass of carbon on the surface is constant, thicker fusion zones lead to lower carbon concentrations. The theoretical amount of carbon in the fusion zone of 1 mm depth, based upon the assumption that during plasma surface treatment all carbon pasted on the surface is introduced in the composition of the alloyed area, is estimated to be equal to 1.1 wt%. It is known that in a martensitic condition carbon increases the hardness of the steel when its content is up to 1.0 wt%, when this limit is exceeded the hardness drops again due to large volumes of retained austenite in the microstructure [21]. Since the maximum FZ depth obtained in this work is 1 mm, with calculated 1.1 wt% carbon, the hardness should be increased as the depth of the FZ increases.

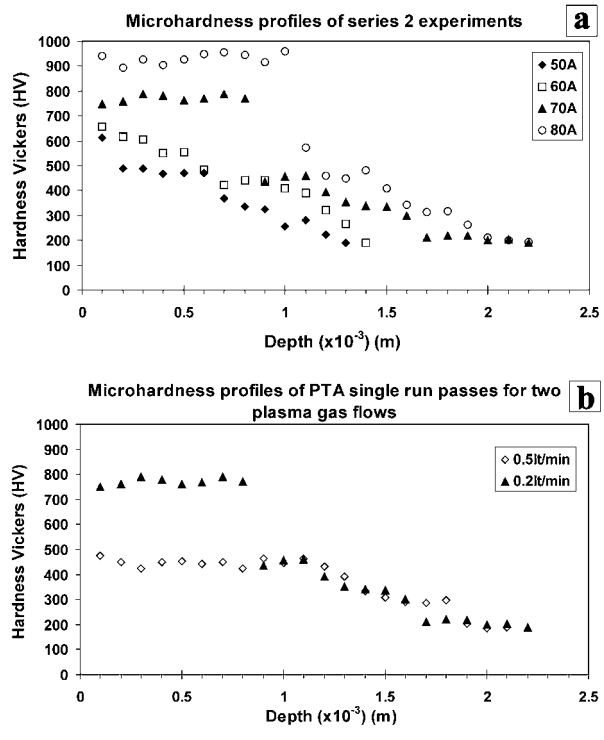

Figure 5 (a) The effect of PTA current in the microhardness profile of the single run plasma passes. (b) The effect of plasma gas flow rate on the microhardness profile of the single run plasma passes (PTA current 70 A).

The hardness of the FZ is also dependent on the plasma gas flow rate and shielding gas flow as it can be seen in Fig. 5b. For a fixed value of PTA current decreasing the plasma gas flow from 0.5 lt/min to 0.2 lt/min leads to higher hardness of the FZ. As mentioned in the previous section a lower plasma gas flow forms more restricted plasma column, which leads to higher energy densities and higher cooling rates. Thus the hardness is higher, Fig. 5b and the heat affected zone is smaller, Fig. 4b.

3.2. Multiple run tests

3.2.1. Microstructure

Based upon the results of the plasma single run experiments a single set of PTA operation parameters (series 2.3) were chosen for scanning a whole surface (PTA current 70 A, PGF 0.2 lt/min and SGF 3.9 lt/min). The parameters chosen produced satisfactory depth of fusion zone (0.8 mm) and high hardness (mean 750 HV). Because the workpieces had relatively small sizes they were placed in a water tank and three surfaces with different cooling conditions were prepared. Surface A with no cooling media, surface B with iced water as cooling media and surface C with water in room temperature as cooling media.

A general view of a cross section of a multiple run surface is presented in Fig. 6a (Surface A). The fusion zone with a mean depth of 1 mm can be seen in the upper region of the micrograph. The FZ is uniform without gas pores or cracks and is well bonded to the substrate material. The absence of pores and cracks is presumably due to the argon gas protection, characteristic of the plasma process and relatively low cooling rates which allows gases to escape from the bath. The HAZ is quite thick (several mm) due to heat saturation of the substrate caused by insufficient cooling.

The microstructure of Surface A was pearlitic with coarse cementite (Fe_3C) particles, Fig. 6b, although in the case of single run experiments the corresponding microstructure of the FZ consisted of martensite. The fusion zone depth obtained was 1 mm, 0.2 mm higher than that of the single run experiment. The carbon content was calculated as in single run experiments, to approximately 1.1 wt% and it was measured with mass spectrography (M.S.) to 1.05 wt%. According to Andrews linear formula [21] the Ms temperature can be estimated to be about 60°C. The continuous heating of the multiple plasma passes raises the bulk temperature above the Ms temperature and martensitic transformation is impossible. XRD examination confirms the metallographic findings revealing that the microstructure of Surface A consists of ferrite and cementite, Fig. 7.

Although, carbon alloying (carburizing) is achieved, hard martensitic microstructures (case hardening) are not produced In order to counteract this difficulty cooling of the substrate material was applied during the process by immersing the metal specimen into a tank containing water and ice, Surface B. Fig. 6c illustrates the microstructure of the fusion zone of Surface B. Martensite needles surrounded by retained austenite and probably some carbides are observed, but small alloying depth was achieved due to the high cooling rate imposed to the substrate metal. The FZ depth is about

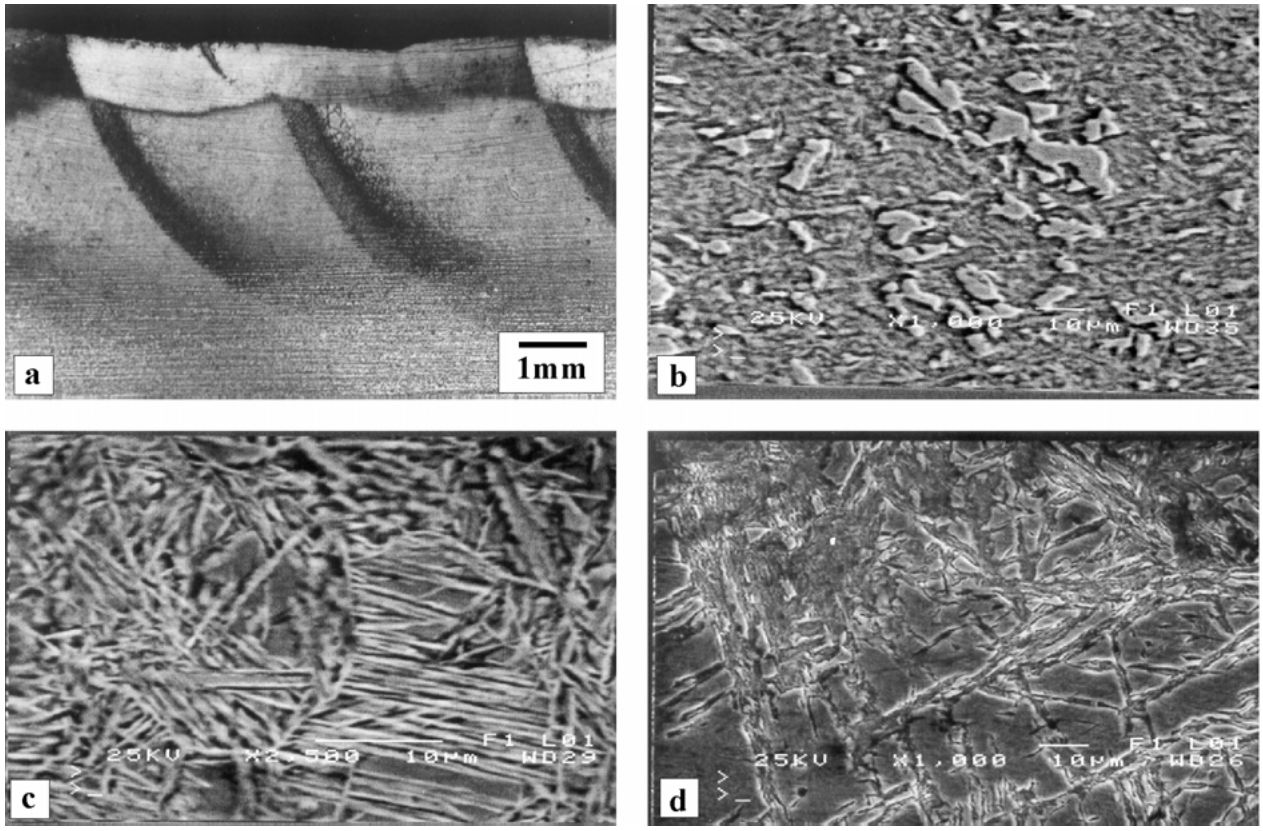

Figure 6 (a) Optical micrograph of a cross section of Surface A. (b), (c), (d) SEM micrographs of the fusion zone showing: the hypereutectoid microstructure of Surface A, the martensitic microstructure of Surface B and the martensitic—bainitic microstructure of Surface C respectively.

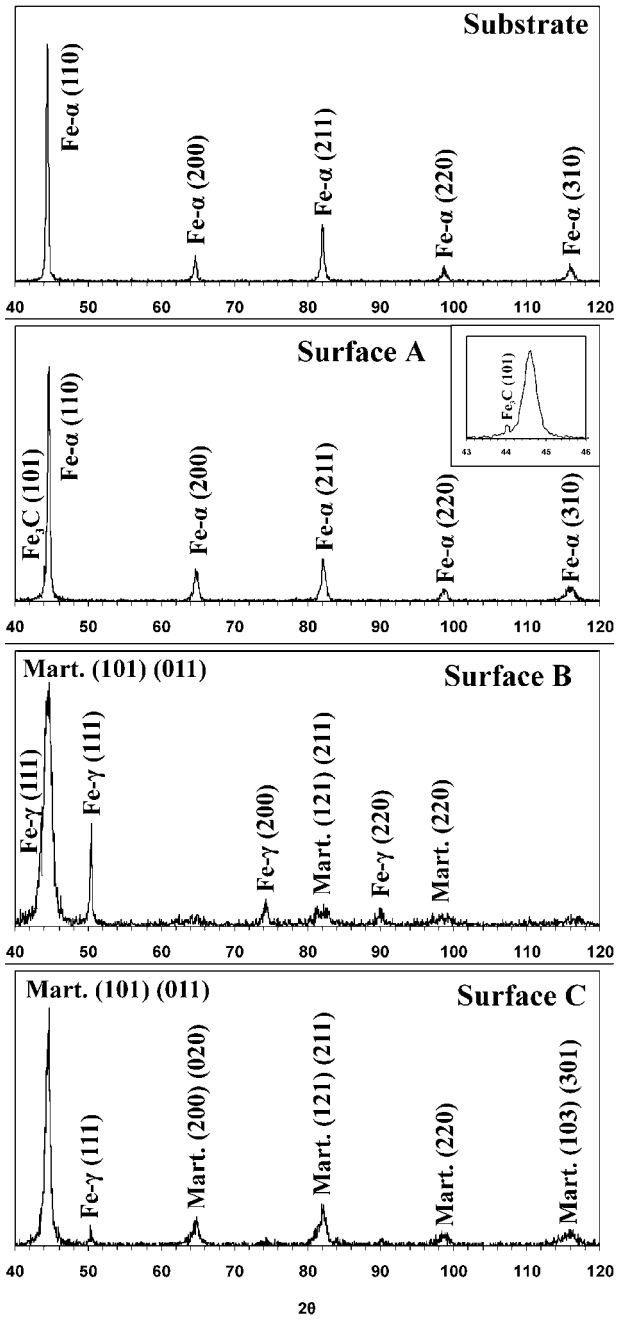

Figure 7 X-ray diffraction of substrate steel and surfaces A through C carburized using the PTA technique.

0.4 mm, 0.4 mm smaller than that of the single run experiment, which leads to a carbon content of 2.4 wt% (calculated). The measurements with mass spectrography showed a carbon level of approximately 2.3 wt%. The XRD examination of the surface showed large amounts of retained austenite and martensite, Fig. 7, as mentioned before.

A third multi-run surface was prepared, Surface C, where the metal was cooled by in room temperature water, Fig. 6d. Martensite and upper-bainite can be seen in the fusion zone with retained austenite also present. The depth of the fusion zone is 0.8 mm, which is exactly the depth of the FZ of the corresponding single run experiment. The carbon content was estimated to 1.3 wt% and was measured with mass spectography to 1.2 wt%. For this level of carbon concentration the amount of retained austenite expected is of the order of 25% to 30% [21] but using the ASTM E975-95 standard, the XRD graph, Fig. 7, reveals considerably lower amounts of austenite, than those previously mentioned. This is due to the beneficial effect of post heat treatment imposed by the subsequent passes on the previous ones.

3.2.2. Microhardness of the surfaces

As mentioned before different cooling conditions resulted in different cooling rates and thus to different microstructures but also in differences in the alloying depth of the plasma surface alloyed layers, Fig. 8a. Surface A had an average hardness in the FZ of 350 HV and an alloying depth of approximately 1 mm. Higher hardness was achieved in the case of Surfaces B and C, where in the FZ an average of 600 HV and 660 HV respectively was measured. While hardness of the two surfaces does not show significant variation, the alloying depth of Surface B, 0.4 mm, is significantly smaller than that of surface C which is 0.8 mm.

A multiple run scanning of a metal with PTA differs from a single run test because each scanning pass is reheated by the subsequent passes to a different degree. This post heating of each scanning pass affects its microstructure and hence its hardness. This fact is clearly shown in Fig. 8b, where the microhardness profile of PTA alloyed surface C is compared to the single run experiment with the same PTA operating parameters. Although the alloying depth is not affected, the average hardness of the FZ is nearly 100 HV less in the case of the multiple run Surface C, compared to the single run test.

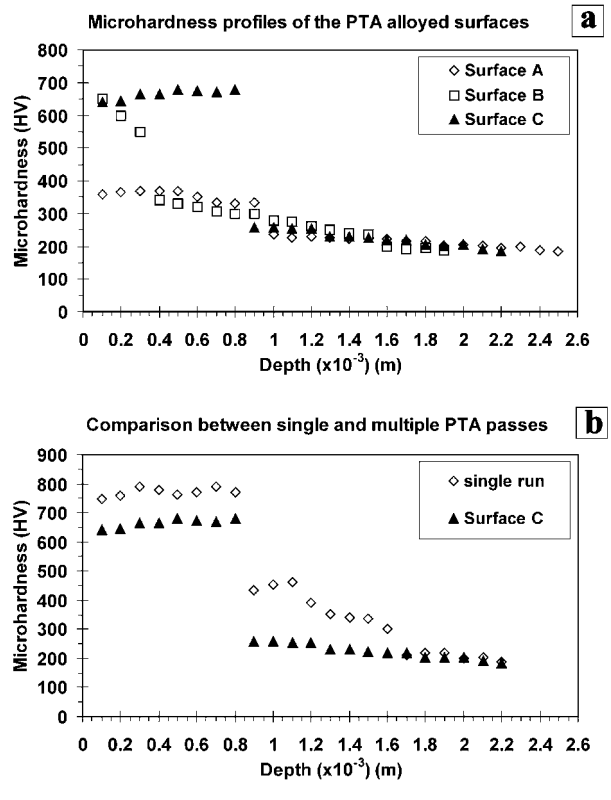

Figure 8 (a) Microhardness profiles of the three surfaces (A, B, C) carburized using the PTA technique. (b) Comparison between single run (series 2.3) and multiple run (Surface C) experiments.

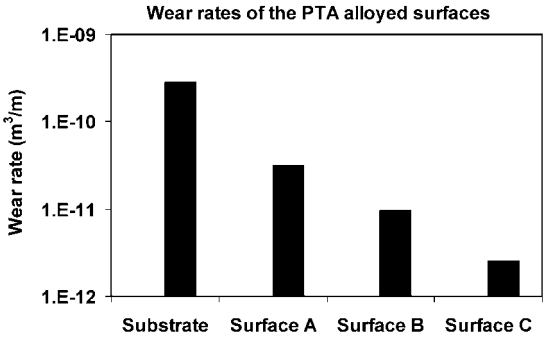

Figure 9 Wear rates of substrate material and the PTA alloyed surfaces under different cooling rates, for an applied load of 9.8 N and sliding velocity of 0.12 m/s.

3.2.3. Wear tests

The plasma transferred arc-alloyed surfaces (A, B and C) and a surface from the substrate material were polished up to 2000 grit emery paper and cleaned with acetone in an ultrasonic bath. The wear tests were done with a pin on disk apparatus (ASTM G99-95a) with counter body a 6 mm diameter Al_2O_3 ball with a hardness of 1900 HV. The rotating part was the under test surface and the conditions applied were 9.8 N load and 0.12 m/s sliding velocity. The wear rate was estimated as volume loss of material per meter sliding distance and is illustrated in Fig. 9. As it was expected the substrate material, low carbon steel with 180 HV hardness, presents the highest wear rate followed by Surface A which is one order of magnitude lower. This is due to the increased hardness of surface A, about 360 HV, two times greater than that of the substrate steel. PTA alloyed surfaces B and C present very low wear rates in relation to substrate steel. Especially the wear rate of surface C is about two orders of magnitude lower than the plain steel. Plasma treated surfaces B, with cooling media iced water, and C with cooling media water at room temperature, have about the same hardness but present different wear behavior, this is due to their different microstructure which was discussed earlier.

The surface damage of the wear tracks of the pin on disk tested surfaces justifies the decreasing order of the wear rate from substrate material and surface A to surface C, Fig. 10. The plain steel track presents vertical cracks to the sliding direction and deep grooves, Fig. 9a, which are evidence of severe plastic deformation (delamination wear) [22, 23]. On the contrary PTA alloyed surface A presents more shallow grooves, Fig. 10b. That is because pearlite has greater resistance in plastic deformation than ferrite. The hard pro-eutectic cementite carbides dispersed in the pearlite matrix, Fig. 6b, also contribute to diminishing the wear rate.

Plasma alloyed surface B wear track is shown in Fig. 10c, the material was removed from the surface in the form of small flakes leaving elliptic pools on polished surface. This is probably the effect of hard—brittle martensite, which has been formed during the rapid cooling of the surface, Fig. 6c. The pin on disk wear track of surface C reveals no grooving marks like surface A or elliptic pieces missing from the surface. In some areas a thin oxide layer has been formed on the track, Fig. 10d, but generally speaking the surface of the track appears to be smooth and clean.

Taking into account the previous discussion only surface C was chosen in order to conduct pin on disk

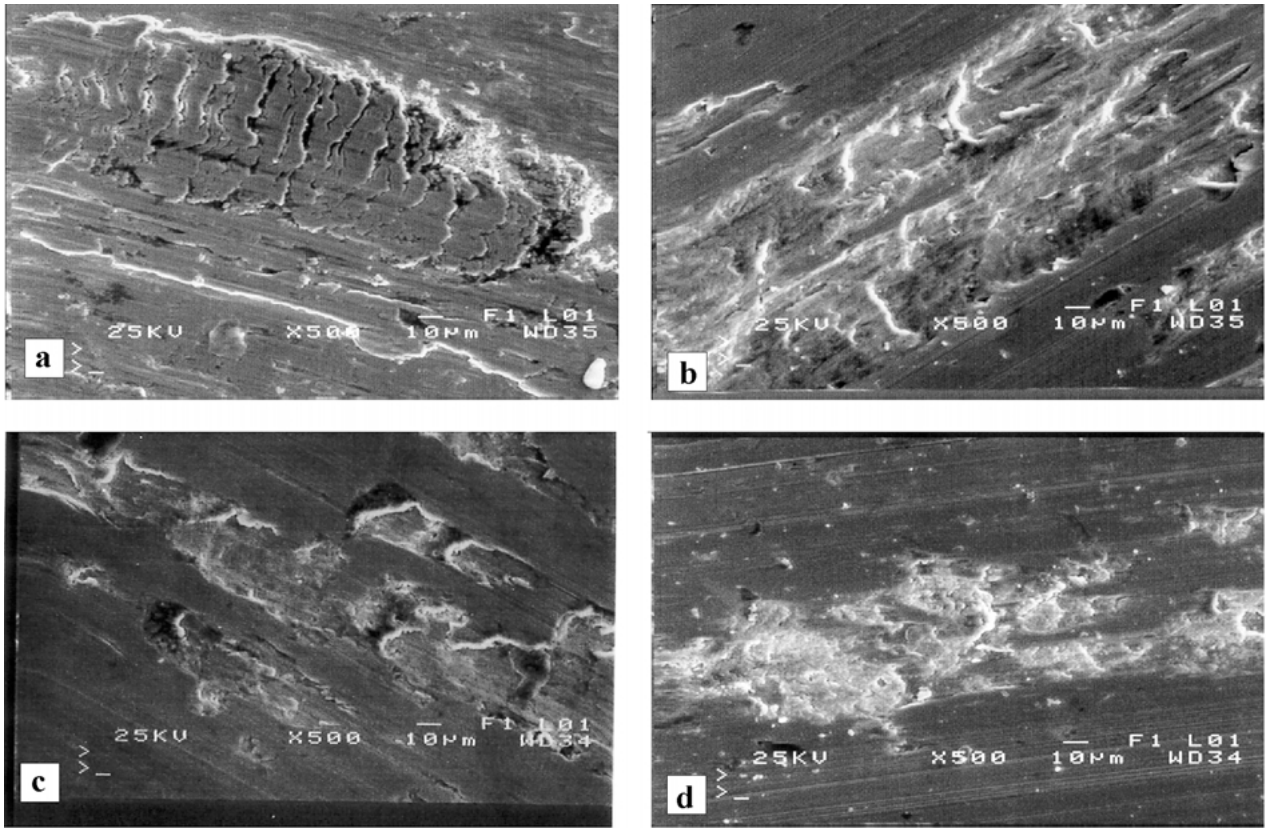

Figure 10 SEM micrographs of the wear tracks of the pin on disk test. (a) Substrate steel, (b) Surface A, (c) Surface B, and (d) Surface C.

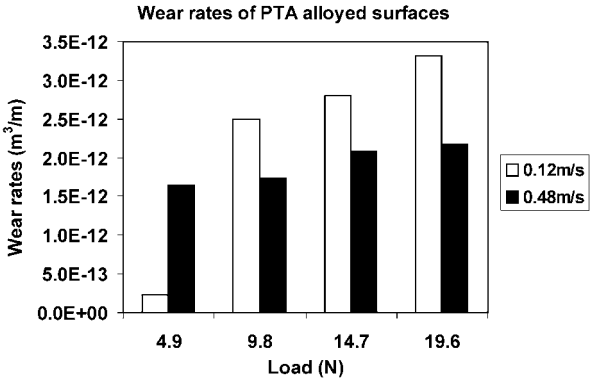

Figure 11 Wear rates of the Surface C under different load and sliding speed conditions.

wear tests under different applied loads (from 4.9 N to 19.6 N) and two different sliding speeds 0.12 m/s and 0.48 m/s. The configuration and procedure followed is the same with the previous mentioned pin on disk tests. The results are illustrated in Fig. 11. For the sliding speed of 0.12 m/s there seems to be a transition between the applied load of 4.9 N and 9.8 N where the wear rate presents one order of magnitude difference. This seems to be a transition between mild to severe plastic deformation wear [24, 25]. Beyond that point the wear rate seems to increase linearly with the applied load. That is also valid for the tests conducted with sliding velocity of 0.48 m/s.

The surface of the wear track of the pin on disk test with applied load 14.7 N and sliding speed of 0.12 m/s, Fig. 12a shows plastic deformation grooves which are covered with an oxide layer revealing that

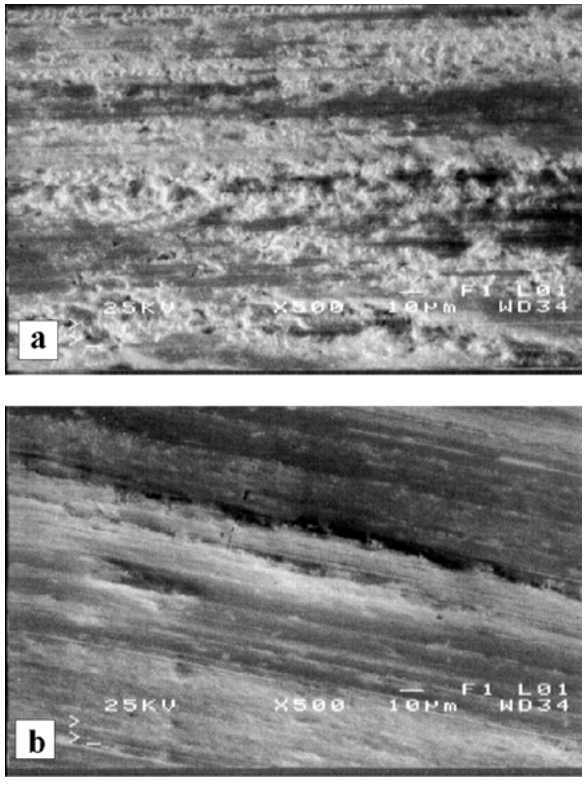

Figure 12 SEM micrographs of the wear tracks of the pin on disk tests of Surface C for applied load 14.7 N and sliding speed (a) 0.12 m/s and (b) 0.48 m/s respectively.

both oxidation—and plastic deformation play an important role as wear mechanisms. On the other hand all wear tracks produced in tests with 0.48 m/s sliding speed present the same topography like that illustrated in Fig. 12b. The whole track is covered by an oxide layer revealing an oxidation mechanism [26, 27]. That is in agreement with Lim and Ashby wear maps [24, 25] that predict a mild oxidation mechanism for that range of speed. The later justify the reduced wear rate of surface C for sliding speed 0.48 m/s in relation to 0.12 m/s (except for the applied load of 4.9 N) presented in Fig. 11.

4. Conclusions

1. With PTA alloying technique selective carburizing and case hardening of plain steel can be achieved to a significant depth.

2. The depth of carburizing can be pre-selected adjusting the PTA operation parameters.

3. The produced alloyed layers are free of pores and cracks and are well bonded to the substrate.

4. Because the carburizing process is held in the liquid state (melt) the carbon content is uniform along the depth of the fusion zone, as it is verified by metallography and microhardness testing. High concentrations of carbon in the fusion zone up to 2.3 wt%, is achieved.

5. According to cooling conditions, either carburizing, with cementite—pearlite microstructure, or case hardening, with quenched and tempered microstructures of carburized layer, are obtained.

6. Wear resistance in all PTA treated samples is considerably improved in relation to the untreated specimen. This is due to the beneficial effect of carburizing which results in an increase of hardness of the PTA treated surfaces.

References

1. K. E. THELNING, in "Steel and Its Heat Treatment" (Butterworths, Boston, 1984) pp. 444, 484.
2. K. H. PRABHUDEV, in "Handbook of Heat Treatment of Steels" (McGraw-Hill, New Delhi, 1988) pp. 302, 341, 343.
3. C. W. DRAPER and C. A. EWING, *J. Mater. Sci.* **19** (1984) 3815.
4. A. WALKER, H. M. FLOWER and D. R. F. WEST, *ibid.* **20** (1985) 989.
5. B. GRÜNENWALD, E. BISCHOFF, J. SHEN and F. DAUSINGER, *Mater. Sci. Technol.* **8** (1992) 637.
6. M. TAYAL and K. MUKHERJEE, *Mater. Sci. Eng.* A **174** (1994) 231.
7. D. K. DAS, *Mater. Character.* **38** (1997) 135.
8. P. CANOVA and E. RAMOUS, *J. Mater. Sci.* **21** (1986) 2143.
9. A. I. KATSAMAS and G. N. HAIDEMENOPOULOS, *Surf. Caot. Technol.* **139** (2001) 183.
10. S. S. SAMOTUGIN, N. KH SOLYANIK and A. V. PUIKO, *Weld. Int.* **9**(6) (1995) 489.
11. S. S. SAMOTUGIN and O. I. NOVOKHATSKAYA, *ibid.* **10**(6) (1996) 495.
12. S. V. PETROV and S. N. KOVAL, *ibid.* **6** (1992) 643.
13. S. S. SAMOTUGIN, *ibid.* **12**(3) (1998) 225.
14. S. S. SAMOTUGIN, A. V. KOVAL' CHUK and V. M. OVCHINNIKOV, *ibid.* **8**(10) (1994) 816.
15. E. N. SAFONOV and V. I. ZHURAVLEN, *ibid.* **12**(4) (1998) 326.
16. M. YAN and W. Z. ZHU, *Surf. Caot. Technol.* **91** (1997) 183.
17. *Idem.*, *Mater. Let.* **34** (1998) 222.

18. M. YAN, *Surf. Coat. Technol.* **99** (1998) 132.
19. M. YAN and W. Z. ZHU, *ibid.* **92** (1997) 157.
20. R. IAKOVOU, L. BOURITHIS and G. PAPADIMITRIOU, *Wear* **255** (2002) 1007.
21. G. KRAUSS, in "Steels, Heat Treatment and Processing Principles" (ASM International, Ohio, 1990) pp. 52, 145.
22. N. P. SHU, *Wear* **25** (1973) 111.
23. *Idem.*, *ibid.* **44** (1977) 1.
24. S. C. LIM and M. F. ASHBY, *Acta Metall.* **35** (1987) 1.
25. S. C. LIM, M. F. ASHBY and J. H. BRUNTON, *ibid.* **43** (1987) 1343.
26. T. F. QUINN, D. M. ROWSON and J. L. SULLIVAN, *Wear* **65** (1980) 1.
27. T. F. QUINN, J. L. SULLIVAN and D. M. ROWSON, *ibid.* **94** (1984) 175.

Received 1 August 2002
and accepted 22 April 2003